Acta Universitatis Sapientiae
Electrical and Mechanical Engineering, 16 (2024) 48–62

DOI: 10.47745/auseme-2024-0005

Comparative Study of Dielectric Properties and Other Physical Properties of Superparamagnetic Iron Oxide Nanoparticles and Polyethylene Nanocomposites

Taraneh JAVANBAKHT[1], Sophie LAURENT[2,3], Dimitri STANICKI[2], Eric DAVID[1]

[1] Department of Mechanical Engineering, École de Technologie Supérieure, Montreal, Quebec, Canada H3C 1K3, Canada,
e-mail: t.javanbakht@gmail.com
[2] Laboratory of NMR and Molecular Imaging, University of Mons, Avenue Maistriau 19, B-7000 Mons, Belgium
[3] Center for Microscopy and Molecular Imaging, 6041 Gosselies, Belgium

Manuscript received, July 04, 2024; revised October 17, 2024

Abstract: The present paper proposes a new investigation of the dielectric properties of superparamagnetic iron oxide nanoparticles (SPIONs)/PE nanocomposites in comparison with the neat polymer at different temperatures. The SPIONs used were without or with positively or negatively surface charge. Different frequency-domain dielectric responses were observed for the different samples. The usual decrease of the values of the real part of the permittivity of all the three SPIONs nanocomposites in the range was observed with the increase of temperature. Moreover, the values of the real part of the permittivity of PE-bare SPIONs increased slightly at lower frequencies, whereas those of PE-positively charged SPIONs and PE-negatively charged SPIONs were constant at higher frequencies and showed an increase at medium frequencies and a plateau at lower frequencies. The imaginary part of their permittivity also showed dielectric responses for the samples.

Keywords: SPIONs, surface charge, physical properties, dielectric properties, functionalization.

1. Introduction

The dielectric properties of non-conductive materials are important physical properties describing their interaction with an external electrical field at frequencies below microwave frequencies [1], [2]. These properties determine the response of materials subjected to an AC electrical field and are relevant in

number of applications such Joule heating, drying or electrostatic energy storage [3], [4].

Polymer nanocomposites are important materials with diverse applications in science and engineering such as for energy storage, sensors and actuators [5], [6], [7]. Efficient, reliable, and affordable production technologies are required for mass production of these materials with stable characteristics [8]. The insertion of metallic or ceramic materials into a matrix, which is usually a polymer, can provide desirable properties for electrical applications [9]. Fabrics [10], buildings [11], and construction materials [11], as well as metallic [12] or polymer [13] matrices can be used for the manufacture of nanomaterials [14]. The dielectric properties of biological materials can be investigated in the interaction of tissues with electromagnetic energy [15], [16]. Physiological changes of the water content, protein content, types and cell structure of biological materials have impact on their dielectric properties. In fact, the dielectric properties of these materials are not identical [17], [18].

During several years, superparamagnetic iron oxide nanoparticles (SPIONs) have found diverse applications in engineering. These nanoparticles are promising because of their magnetic properties, high biocompatibility, and easy functionalization of their surfaces with target molecules [19]. They have diverse physicochemical and mechanical properties that make them usable alone or as nanocomposites, which are often prepared in mixtures with polymers [20], [21], [21]. SPIONs can be classified into three categories: first category with micrometer-sized (300–3.5 μm), second category with standard-sized (10–150 nm), and third category that is ultra-small (<10 nm). Their magnetic properties allow their application for direct delivery of matter into the pathogen zone that does not influence the whole organism [22], [23]. The functionalization of these nanoparticles with organic and inorganic materials is required for their diverse applications in science and engineering. The core part of nanoparticles can be coated with an organic or inorganic layer [20], [21] or/and encapsulated in a polymer-based matrix [21].

The objective of the current work was to investigate the dielectric properties and other physical properties of SPIONs with low density polyethylene (LDPE) nanocomposites. Our hypothesis was that the dielectric properties of SPIONs depended on their surface charge. This study was required for performing a further step in an upcoming comparative investigation on the change of the dielectric properties of SPIONs with other polymeric matrices.

To the authors' knowledge, this comparative investigation on these nanocomposites having no surface charge, positive or negative surface charge on their nanoparticles has not been carried out, yet. The results of this study can be applied for the design and development of new electrical insulation and mechanical support systems.

2. Materials and Methods

A. Samples preparation

SPIONs were premixed with the PE powder in a 2:100 weight ratio. PE/SPIONs composites were then prepared by melt compounding, the premixed LDPE/SPIONs being extruded in a twin-screw extruder and pelletized. Then, the samples were molded using with heating press at 160 °C. Disk-shaped molded samples were used for broadband dielectric spectroscopy (BDS) characterization.

B. Transmission electron microscopy (TEM)

A Microscope Fei Tecnai 10 operating at an accelerating voltage of 100 kV (Oregon, OR, USA) was used for TEM imaging. The samples were prepared on carbon-coated copper-grids (Formvar/carbon 300 mesh; Cu TED PELLA) by placing a 4 µL drop of 0.5 mM suspension (IONPs in water), allowing the liquid to dry at room temperature. The iTEM (Münster, Germany) was used for the statistical treatment of the TEM images. The particles' diameters were measured for the calculation of the mean diameter, the standard deviation and the polydispersity index (PDI). Between 500 and 700 nanoparticles were counted.

C. Thermogravimetric analysis (TGA)

A Pyris Diamond thermogravimetric analyzer (TG/DTA), PerkinElmer technology, Shelton, CT, USA) was used to determine the thermal degradation of the materials and quantify the weight percentage of the inorganic content. Samples were heated from 50°C to 600°C at a rate of 10 °C/min under a nitrogen flow of 100 ml/min.

D. Scanning electron microscopy (SEM)

Cross-sections of the samples were used for SEM imaging and ton dispersive spectroscopy (EDS) measurements, that were carried out with a HITACHI SU8230 SEM. Coating of samples with Pt was performed before SEM imaging to avoid charging effects.

E. Broadband Dielectric Spectroscopy (BDS) measurements

A dielectric frequency-domain spectrometer was used for the measurement of the dielectric response of the samples [20]. Isothermal measurements were conducted in a frequency range from 0.1 to 10^6 Hz at temperature varying from 20 °C to 100 °C. The dielectric properties of the nanocomposites of PE-SPIONs and PE were measured in triplicate. The energy of activation of the interfacial relaxation mechanism was obtained using the linear least squares analysis from the plots of [ln(frequency)] versus [1000/T]. The frequency values for which the

imaginary permittivity values was maximum were considered for the plots [24], [25].

3. Results and Discussion

Fig. 1 shows the TEM images of SPIONs. The average sizes of bare SPIONs, positively charged SPIONs, and negatively charged SPIONs were 7.84 +/- 2.61 nm, 8,38 +/- 2.33 nm, and 8,53 +/- 2.25 nm, respectively.

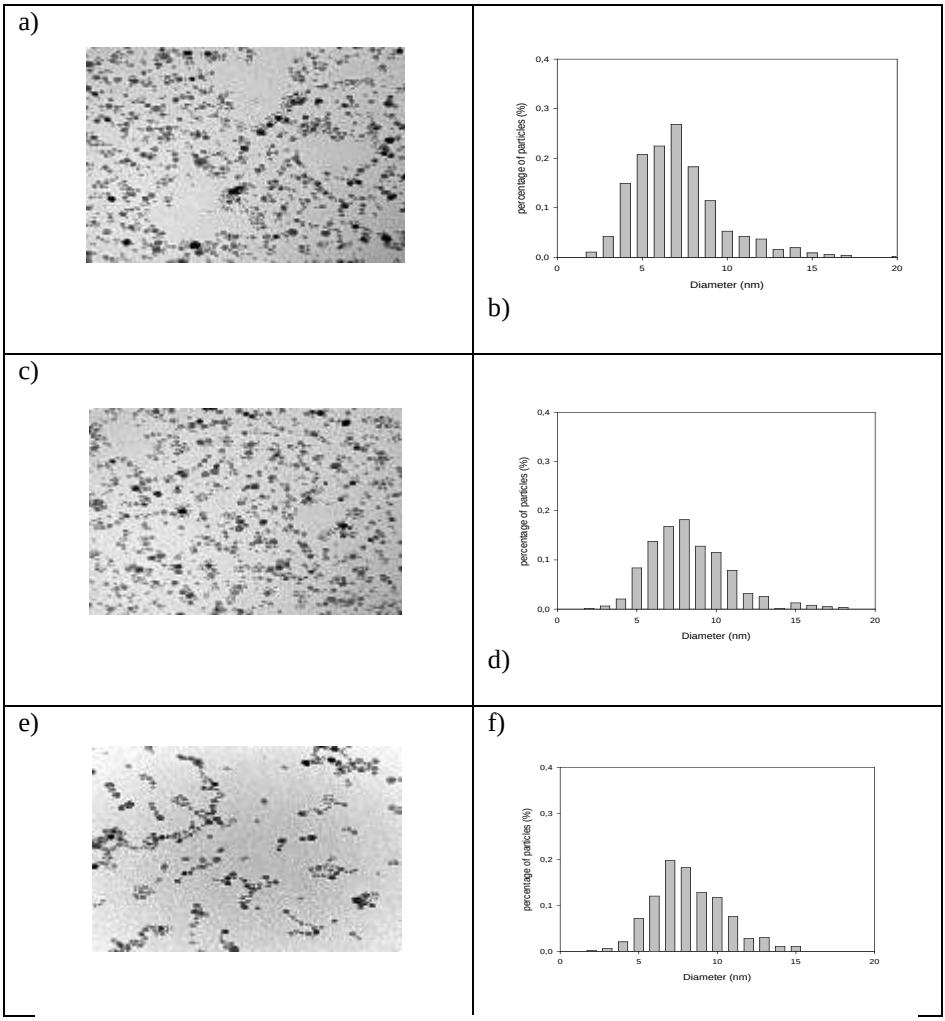

Figure 1: TEM images of a, b) bare SPIONs, c, d) positively charged SPIONs, and e, f) negatively charged SPIONs

Fig. 2 shows the TGA curves of samples. The curves of PE-bare SPIONs, PE-positively charged SPIONs, PE-negatively charged SPIONs, and PE are represented with red line, green line, blue line, and black line, respectively.

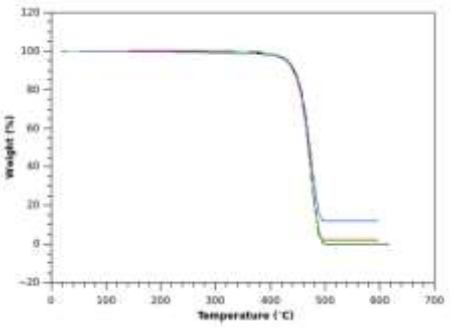

Figure 2: TGA curves of PE-bare SPIONs, PE-positively charged SPIONs, PE-negatively charged SPIONs, and PE in red, green, blue, and black line, respectively. The weight loss percentage indicated in the y-axis was from 100% to 0% for all samples

As shown in *Fig. 2*, all samples burnt in the 400-500°C range. Comparing the weight loss curves, all samples decomposed in a single step. The peak temperature of decomposition for PE-bare SPIONs, PE-positively charged SPIONs, PE-negatively charged SPIONs, and PE were at 470 °C, 470 °C, 470 °C, and 472.6 °C, respectively. Taking into account the heating rate, which was 10 °C/min, the presence of SPIONs in the nanocomposites of PE-SPIONs did not have a significant influence on the temperature of decomposition of these nanocomposites in comparison with that of the polymer.

Table 1 shows the residual weight percentage of samples. As expected, the residual weight percentages of the nanocomposites of SPIONs-PE were more than that of PE alone. Moreover, the PE-bare SPIONs and the PE-negatively charged SPIONs had almost the same residual weight percentages, that were more than that of the PE-positively charged SPIONs.

Fig. 3 and *Fig. 4* show the SEM images and EDS spectra of PE-bare SPIONs, PE-positively charged SPIONs, PE-negatively charged SPIONs and PE. The pics of Pt in the EDS spectra correspond to the coating of samples. The images of samples, C, O, Si and Fe are in grey, red, green, blue, and orange, respectively. Some traces of Na were also found on the surface of the last sample.

The amount of iron was more on the surface of PE-bare SPIONs in comparison with other nanocomposites. Its amount was the least for the PE-negatively charged SPIONs. The amount of O was the most for this last nanocomposite and the least for PE-positively charged SPIONs.

Table 1: The residual weight percentage of samples

Sample	Residual weight (%)
PE-bare SPIONs	2.109
PE-positively charged SPIONs	1.190
PE-negatively charged SPIONs	2.000
PE	0.027

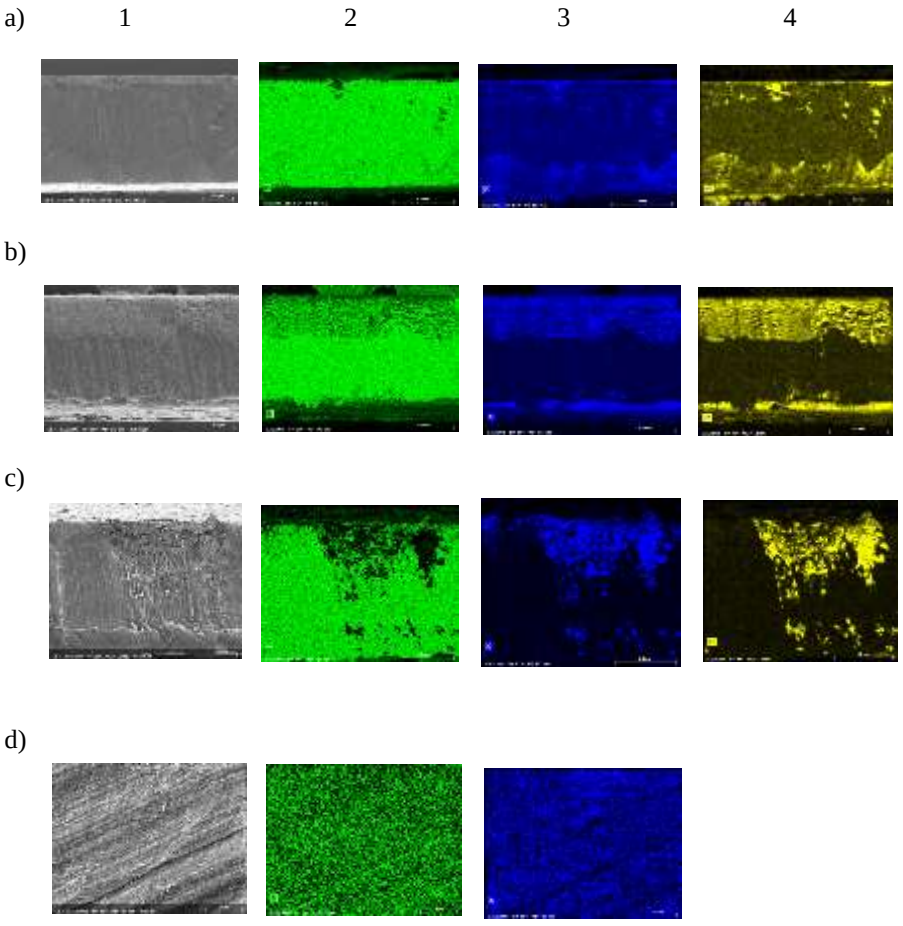

Figure 3: The SEM images of (a) PE-bare SPIONs, (b) PE-positively charged SPIONs, (c) PE-negatively charged SPIONs, and (d) PE. Carbon, oxygen and iron on the surface of samples are observed in green, blue and yellow in the images of the columns 2, 3 and 4, respectively

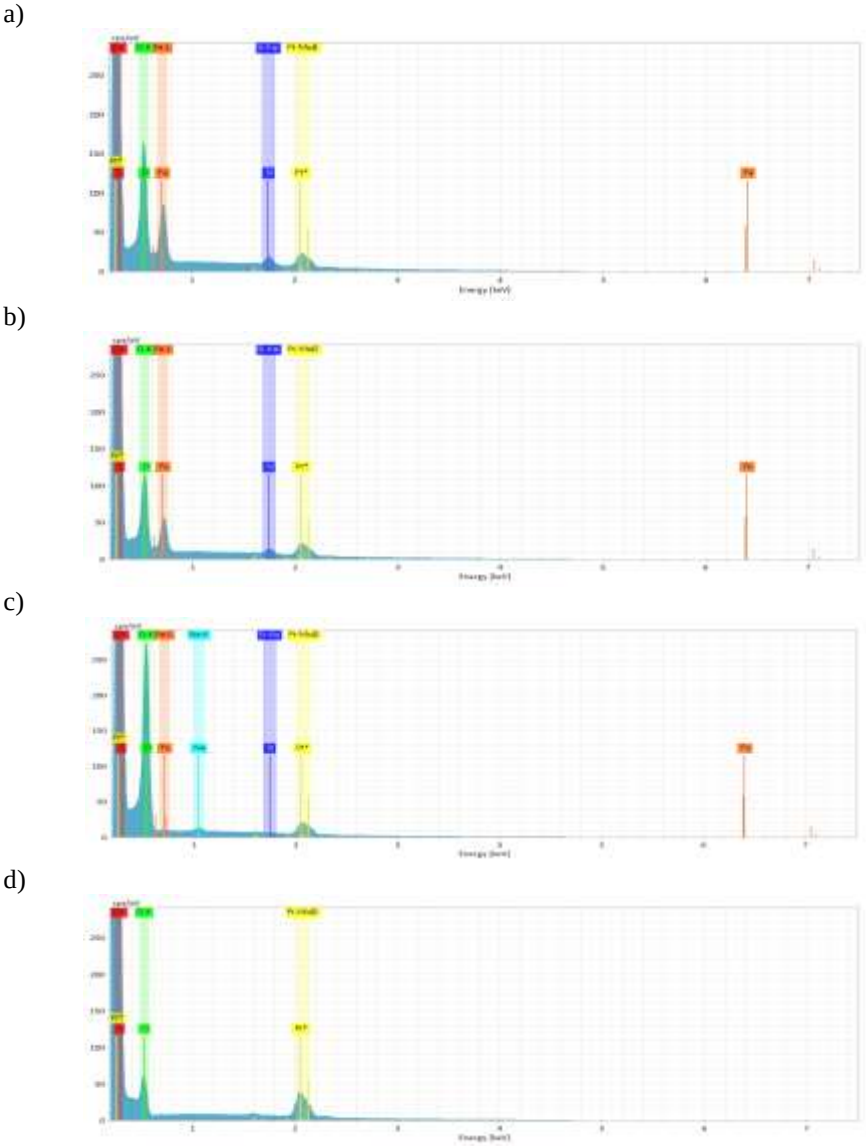

Figure 4: The EDS spectra of (a) PE-bare SPIONs, (b) PE-positively charged SPIONs, (c) PE-negatively charged SPIONs, and (d) PE

Fig. 5 shows the real and imaginary parts of the relative permittivity of PE-bare SPIONs, PE-positively charged SPIONs, PE-negatively charged SPIONs and PE at different temperatures.

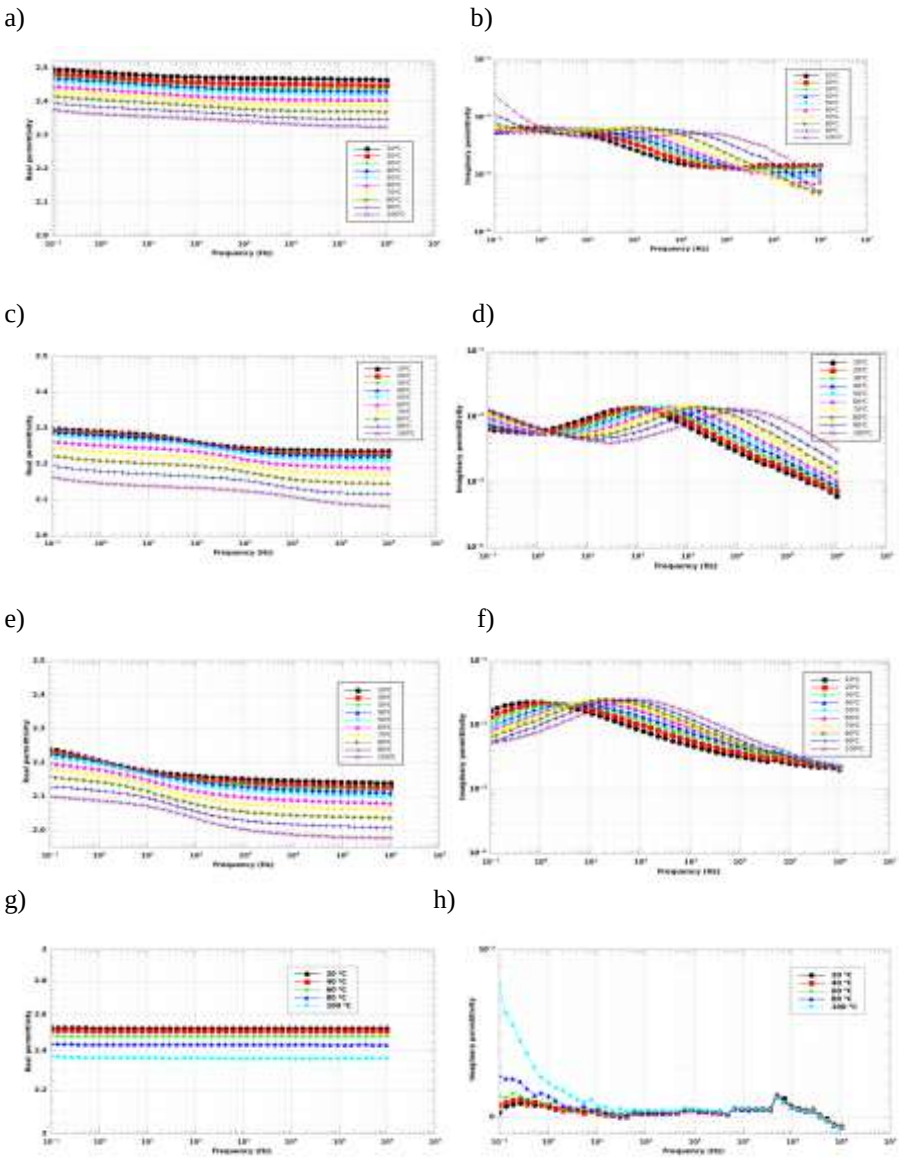

Figure 5: The real part and imaginary part of the relative permittivity of the nanocomposites of (a) and (b) PE-bare SPIONs, (c) and (d) PE-positively charged SPIONs, (e) and (f) PE-negatively charged SPIONs and (g) and (h) PE at different temperatures

As shown in *Fig. 5*, the values of the real part of the permittivity of all the three nanocomposites of SPIONs-PE and of neat PE were found to decrease with the increase of temperature, as expected and in agreement with the Clausius-Mossotti equation. The dielectric response of neat PE showed its usual low-loss dielectric response presenting a rather frequency-independent behavior (known as flat loss behavior [26]) excepted at the highest temperature where charge fluctuations lead to an increase of the dielectric losses towards low frequencies. For all SPIONs composites, containing either bare, positively and negatively charged SPION, a relaxation mechanism, in the form of a temperature dependant loss peak, was observed due to the interfacial polarization between the non-conductive matrix and the more conductive particles. The frequency position of this peak is essentially inversely proportional to the effective conductivity of the filler. Indeed, solving the Laplace equation for a dilute dispersion of ellipsoids (the so-called Maxwell approximation) leads to the following expression for the effective complex permittivity of the composition [27]:

$$\sum_{j=1}^{2} q_j \cdot \left(\hat{\varepsilon}_c - \hat{\varepsilon}_j\right) \cdot \left[1 + A \cdot \frac{\hat{\varepsilon}_j - \hat{\varepsilon}_1}{\hat{\varepsilon}_1}\right]^{-1} = 0\,, \tag{1}$$

where j denotes the phase, q the volume fraction of each phase, the relative complex permittivity and A is a geometrical factor known as the depolarization factor (A = 1/3 for a sphere). Assuming the both filler and matrix complex permittivity can be simply expressed by a real permittivity and a conductivity $\varepsilon = \varepsilon - j\frac{\sigma}{\omega\varepsilon_o}$ then the above equation reduces to a Debye-type process:

$$\varepsilon_c = \varepsilon_\infty + \frac{\Delta\varepsilon}{1 + j\omega\tau}\,. \tag{2}$$

With the retardation (or relaxation) time inversely proportional to the filler's conductivity:

$$T \propto \frac{\varepsilon_0}{\sigma_f}\,. \tag{3}$$

The above approach can be extended to consider the presence of an interfacial layer between the filler particles and the matrix material [28]. In that case, the retardation time will be rather related to the conductivity of the interfacial layer [28]. A common case where this situation occurs is when a water layer is present on the surface of a hydrophilic filler [29]. In all cases, the retardation time of the loss peak was found to decrease with the increase of temperature, indicating an increase of either filler of interfacial layer conductivity.

Fig. 6 shows the imaginary part of the relative permittivity of the nanocomposites of PE-SPIONs at 10 °C and 100 °C.

(a)

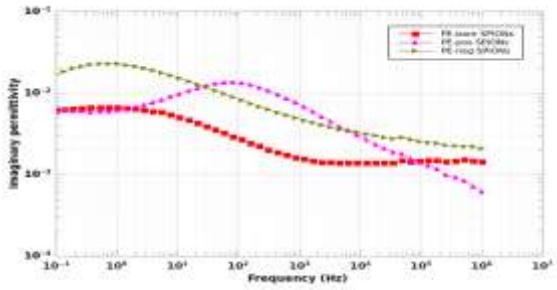

(b)

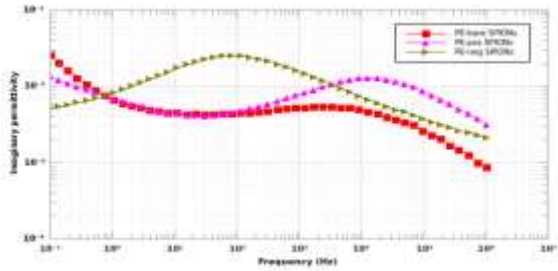

Figure 6: The imaginary part of the relative permittivity of the nanocomposites of PE-SPIONs at 10 °C and 100 °C

The local maximum shift was observed for the imaginary part of the relative permittivity of the nanocomposites of PE-SPIONs for each temperature in *Fig. 6*.

Fig. 7 shows the relaxation rate of the interfacial processes as function of the inverse temperature for the three composites. In all cases the activation plot is in good agreement with an Arrhenius-type thermal activation.

a)

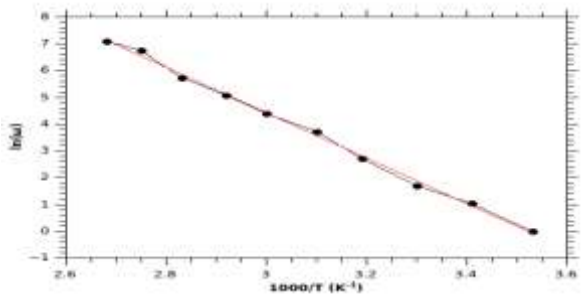

b)

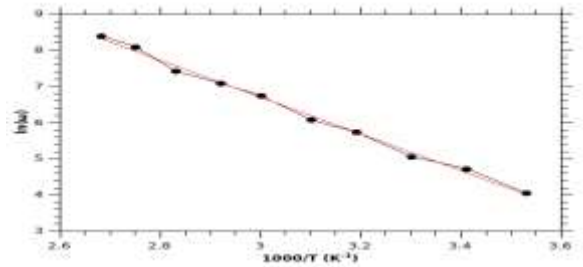

c)

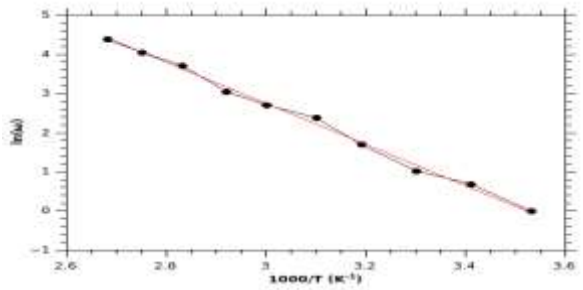

Figure 7: The Arrhenius plots of a) PE-bare SPIONs, b) PE-positively charged SPIONs and c) PE-negatively charged SPIONs.

The slopes were used to determine the energy of activation for the relaxation process of samples. Activation energies determined from the slope of the plots were 69.6 kJ/mol, 45.5 kJ/mol and 40.8 kJ/mol for PE-bare SPIONs, PE-positively charged SPIONs and PE-negatively charged SPIONs, respectively. This showed that the values of the energy of activation of the relaxation process for the nanocomposites of SPIONs were not identical, with the activation energy of PE-bare SPIONs significantly higher than for the two other composites.

The decrease of relative permittivity in nanocomposites has been attributed to the interaction between the polymer matrix and the nanoparticles [29].

The low-density region and the less stoichiometric region form the interaction zone, which has an increased free volume and some traps. The study with a multi-core model consisting of a bonded region, a transition region and a normal region showed that the nanoparticles can be considered as isolated particles as they provide slight filler loading [30], [31], 32]. When the movement of orientable dipoles are restricted along the direction of the electric field, the relative permittivity is decreased. When more concentrations of nanoparticles load the matrix, the distance between neighboring nanoparticles decreases that can result in the overlap of the transition regions of neighboring nanoparticles. This phenomenon has impact on the dielectric properties of nanocomposites. The relative permittivity of nanoparticles is higher than that of the polymer, which results in the higher relative permittivity of nanocomposite [29], [33], [34]. The obtained data will be computed with modeling in a further work.

Several other materials alone or with polymers have been investigated for their physicochemical [35], [36], biological [37], [38], [39] and mechanical properties [40], [41], [42]. The analysis of their dielectric properties would be required for a better development of their preparation. The consideration of the physical properties of these materials as those of PE-SPIONs without and with surface charge as described above leads to promise for their applications.

4. Conclusion

This study was focused on the analysis of the dielectric and other physical properties of the PE-SPIONs nanocomposites. The dielectric properties of the composite samples were dominated by the presence of an interfacial polarization process exhibiting an Arrhenius-type thermal activation. Significant differences were found between the bare, positively, and negatively charged SPIONs due to the different surface chemistry. The current work also revealed that the values of the real part of the permittivity of PE-bare SPIONs increased slightly at lower frequencies, whereas those of PE-positively charged SPIONs and PE-negatively charged SPIONs were constant at higher frequencies and showed an increase at medium frequencies and a plateau at lower frequencies. More investigation will lead to the development of these materials for their applications in science and engineering.

Acknowledgements

We acknowledge the financial support from NSERC (Alliance International grant) for the support of this work.

References

[1] Nelson, S.O. “Dielectric properties of materials and measurement techniques”, *Drying Technology*, vol. 8, pp. 1123–1142, 1990.

[2] Nelson, S.O., Trabelsi, S. “Factors influencing the dielectric properties of agricultural and food products”, *Journal of Microwave Power and Electromagnetic Energy*, vol. 46, pp. 93–107, 2012.

[3] Musa, N. et al. “Frequency and temperature dependence of ethanol using the cole-cole relaxation model”, *American Journal of Condensed Matter Physics*, vol. 10, pp. 44–49, 2020.

[4] Kannan, S. et al. “The effect of radiofrequency heating on the dielectric and physical properties of eggs”, *Progress In Electromagnetics Research B*, vol. 51, pp. 201–220, 2013.

[5] Shivashankar, H. et al. “Investigation on dielectric properties of PDMS based nanocomposites”, *Physica B: Condensed Matter*, vol. 602, 412357, 2021.

[6] Sadasivuni, K.K. et al. “A review on porous polymer composite materials for multifunctional electronic applications”, *Polymer-Plastics Technology and Materials*, vol. 58, pp. 1253–1294, 2019.

[7] Elhi, F. et al. “Cellulose-multiwall carbon nanotube fiber actuator behavior in aqueous and organic electrolyte”, *Materials*, vol. 13, 3213, 2020.

[8] Getmanov, A.G., Thang, T.Q. “Dielectric properties of nanocomposites based on epoxy resins and titanium dioxide”, *International Journal of Circuits, Systems and Signal Processing*, vol. 15, pp. 1400–1406, 2021.

[9] Ciobanu, R.C. et al. “Simulation of dielectric properties of nanocomposites with non-uniform filler distribution”, *Polymers*, vol. 15, 1636, 2023.

[10] Wang, Y., Gordon, S., Baum, T., Xu, Z. “Multifunctional stretchable conductive woven fabric containing metal wire with durable structural stability and electromagnetic shielding in the x-band”, *Polymers*, vol. 12, 399, 2020.

[11] Akyıldız, A., Durmaz, O. “Investigating electromagnetic shielding properties of building materials doped with carbon nanomaterials”, *Buildings*, vol. 12, 361, 2022.

[12] Carneiro, Í., Simões, S. “Effect of morphology and structure of MWCNTs on metal matrix nanocomposites”, *Materials*, vol. 13, 5557, 2020.

[13] Moskalyuk, O.A., Belashov, A.V., Beltukov, Y.M., Ivan’kova, E.M., Popova, E.N., Semenova, I.V., Yelokhovsky, V.Y., Yudin, V.E. “Polystyrene-based nanocomposites with different fillers: Fabrication and mechanical properties”, *Polymers*, vol. 12, 2457, 2020.

[14] Ali, A., Mitra, A., Aïssa, B. “Metamaterials and metasurfaces: A review from the perspectives of materials, mechanisms and advanced metadevices”, *Nanomaterials*, vol. 12, 1027, 2022.

[15] Pethig, R. “Dielectric properties of biological materials: Biophysical and medical applications”, *IEEE Transactions on Electrical Insulation*, vol. 1-19, pp. 453–474, 1984.

[16] Wang, X., et al. “High-resolution probe design for measuring the dielectric properties of human tissues”, *Biomedical Engineering*, vol. 20, 86, 2021.

[17] Wang, Z. “*Research and application of microwave method for measuring electrical parameters of biological tissue* (in Chinese)”, Nanjing: Nanjing University of Science and Technology, 2009.

[18] Yilmaz, T, Kılıç, MA, Erdoğan, M, et al. “Machine learning aided diagnosis of hepatic malignancies through in vivo dielectric measurements with microwaves”, *Phys. Med. Biol.*, vol. 61, pp. 5089–102, 2016.

[19] Xie, W., Guo, Z., Gao, F., Gao, Q., Wang, D., Liaw, B., Cai, Q., Sun, X., Wang, X., Zhao, L. “Síntesis controlada por forma, tamaño y estructura y biocompatibilidad de nanopartículas de óxido de hierro para teranóstica magnética”, *Theranostics*, vol. 8, pp. 3284–3307, 2018.

[20] Javanbakht, T., Laurent, S., Stanicki, D., David, E. "Related physicochemical, rheological, and dielectric properties of nanocomposites of superparamagnetic iron oxide nanoparticles with polyethyleneglycol", *Journal of Applied Polymer Science*, vol. 136, pp. 48280–48290, 2019.
[21] Javanbakht, T., Laurent, S., Stanicki, D., Frenette, M. "Correlation between physicochemical properties of superparamagnetic iron oxide nanoparticles and their reactivity with hydrogen peroxide", *Canadian Journal of Chemistry*, vol. 98, pp. 601–608, 2020.
[22] Seabra, A., Pelegrino, M., Haddad, P. "Antimicrobial applications of superparamagnetic iron oxide nanoparticles: Perspectives and challenges", In Nanostructures for Antimicrobial Therapy, 1st ed.; Ficai, A., Grumezescu., A.M., Eds., Elsevier Inc.: Cham, Switzerland, pp. 531–550, 2017.
[23] Bustamante-Torres, M. et al. "Polymeric composite of magnetite iron oxide nanoparticles and their application in biomedicine: A review", *Polymers*, vol. 14, 752, 2022.
[24] Fanari, F. et al. "Broadband dielectric spectroscopy (BDS) investigation of molecular relaxations in durum wheat dough at low temperatures and their relationship with rheological properties", *Food Science and Technology*, vol. 16, 113345, 2022.
[25] Boned, C., Lagourette, B., Clausse, M. "Dielectric behaviour of ice microcrystals: A study versus temperature", *Journal of Glaciology*, vol. 22, pp. 145–154, 1979.
[26] Jonscher, A.K. "*Universal Relaxation Law*", Chelsea Dielectric Press, London, 1996.
[27] Torquato, S. "Random Heterogeneous Materials", Springer, 2002.
[28] Steeman, P.A.H., Maurer, F.H.J. "An interlayer model for the complex dielectric constant of composites", *Colloid and Polymer Science*, vol. 268, pp. 315–325, 1990.
[29] Couderc, H., David, E., Fréchette, M. "Study of Water Diffusion in PE-SiO_2 Nanocomposites by Dielectric Spectroscopy", *Trans. on Electrical and Electronic Materials*, vol. 15, pp. 291–296, 2014.
[30] Tanaka, T., Montanari, G.C., Malhaupt, R. "Process, understanding and challenges in the field of nanodielectrics", *IEEE Trans. Dielectr. Electr. Insul.*, vol. 11, pp. 763–784, 2004.
[31] Tanaka, T., Kozako, M., Fuse, N., Ohki, Y. "Proposal of a multi-core model for polymer nanocomposite dielectrics", *IEEE Trans. Dielectr. Electr. Insul.*, vol. 12, pp. 669–681, 2005.
[32] Zhao, W., Fan, Y., Chen, H. "Dielectric properties and corona resistance of Si-B/epoxy nano-composites", *J. Mater. Sci. Mater. Electron.*, vol. 30, pp. 16298–16307, 2019.
[33] Hardoň, S. et al. "Influence of nanoparticles on the dielectric response of a single component resin based on polyetherimide", *Polymers*, vol. 14, 2202, 2022.
[34] Zhou, C. et al. "Improving the dielectric properties of polymers by incorporating nanoparticles", *10th International Conference on Electrical Insulation* (INSUCON), Birmingham, 2006.
[35] Djavanbakht, T., Carrier, V., André, J. M., Barchewitz, R., Troussel, P. "Effets d'un chauffage thermique sur les performances de miroirs multicouches Mo/Si, Mo/C et Ni/C pour le rayonnement X mou" Journal de Physique IV, France, vol. 10, pp. 281–287, 2000.
[36] Javanbakht, T., Hadian, H., Wilkinson, K. J. "Comparative study of physicochemical properties and antibiofilm activity of graphene oxide nanoribbons", *Journal of Engineering Sciences*, vol. 7(1), pp. C1–C8, 2020.
[37] Wetteland, C.L., Liu, H. "Optical and biological properties of polymer-based nanocomposites with improved dispersion of ceramic nanoparticles", *Journal of Biomedical Materials Research*, vol. 106, pp. 2692–2707, 2018.
[38] Javanbakht, T., Sokolowski, W. "Thiol-ene/acrylate systems for biomedical shape-memory polymers", *Shape Memory Polymers for Biomedical Applications*, pp. 157–166, 2015.
[39] Javanbakht, T., Ghane-Motlagh, B., Sawan, M. "Comparative study of antibiofilm activity and physicochemical properties of microelectrode arrays", *Microelectronic Engineering*, vol. 229, 111305, 2020.

[40] Modal, D., Willett, T.L. “Mechanical properties of nanocomposite biomaterials improved by extrusion during direct ink writing”, *Journal of Mechanical Behavior of Biomedical Materials,* vol. 104, 103653, 2020.

[41] Javanbakht, T., David, E. “Rheological and physical properties of a nanocomposite of graphene oxide nanoribbons with polyvinyl alcohol”, *Journal of Thermoplastic Composite Materials,* 0892705720912767, 2020.

[42] Kostas, V. et al. Synthesis, “Characterization and mechanical properties of nanocomposites based on novel carbon nanowires and polystyrene”, Applied Sciences, vol. 10, 5737, 2020.